

Accurate structure-based coarse-graining leads to consistent barrier-crossing dynamics

Tristan Bereau* and Joseph F. Rudzinski

Max Planck Institute for Polymer Research, 55128 Mainz, Germany

(Dated: December 27, 2018)

Structure-based coarse-graining of molecular systems offers a systematic route to reproduce the many-body potential of mean force. Unfortunately, common strategies are inherently limited by the molecular-mechanics force field employed. Here we extend the concept of multisurface dynamics, initially developed to describe electronic transitions in chemical reactions, to accurately sample the conformational ensemble of a classical system in equilibrium. In analogy to describing different electronic configurations, a surface-hopping scheme couples distinct conformational basins beyond the additivity of the Hamiltonian. The incorporation of more surfaces leads systematically toward improved cross-correlations. The resulting models naturally achieve consistent long-time dynamics for systems governed by barrier-crossing events.

The complex separation of length- and time-scales in soft-matter systems calls for modeling strategies at different resolutions: from quantum, to classical atomistic, to mesoscopic, to the continuum scale [1–4]. Among them, particle-based coarse-grained (CG) models, which try to remain close to the chemistry while averaging over the faster degrees of freedom, have offered significant insight into complex (bio)molecular systems [5–8]. These models shine through both an effective reductionist approach to testing what interactions lead to reproducing certain phenomena, and a significant computational speedup to tackle systems prohibitively large at the atomistic scale.

Instead of targeting a potential energy surface, averaging over degrees of freedom leads to a many-body potential of mean force (MB-PMF) [9, 10]. While several systematic methods exist to target the MB-PMF [9, 11–13] their accuracy tends to be limited not by the performance of the method, but rather by the molecular-mechanics terms used to approximate the MB-PMF. Several recent attempts have been made at using more complex interaction terms [14–16], illustrating the need for more accurate models. In this Letter, we present a unique strategy for generating complex cross-correlations between interaction terms of a force field, thereby accurately recovering the MB-PMF. We analyze the structural and dynamical properties of CG models in the limit of accurately matching these cross-correlations.

Limitations of the molecular-mechanics force field have long been addressed for chemical reactions by methods such as empirical valence bond [17], its multisurface extension [18], and surface-hopping schemes [19]. In these approaches, reactions are effectively decomposed into surfaces with distinct electronic configurations, such as the two bonded states for a proton transfer. The limitations of the force-field interaction terms are overcome by coupling distinct potential energy surfaces (PESs) through surface-hopping dynamics.

In the classical simulation community, researchers have coupled distinct force fields to describe internal-state conversions of coarse-grained units [20], entanglement in

polymer melts [21], and large-scale conformational transitions of biomolecules [22]. In the case that the force-field interaction functions can be expressed analytically as a function of a continuous order parameter, e.g., in dissipative particle dynamics models with local density-dependent potentials [23], no explicit hopping protocol is required, as the dynamics along the continuous hypersurface of force fields is well-defined by the normal integration scheme. On the other hand, if switching between force fields is discrete and, in particular, if a timescale separation exists between force-field transitions and the local motion of particles, Monte Carlo provides a robust route for instantaneous switching between force fields. Voth and coworkers have recently laid out an elegant “ultra coarse-graining” framework in this context, where conversions between discrete internal states are modeled by stochastic transitions between distinct force fields [24, 25].

In the present work, we expand upon previous efforts by considering the common situation where significant coupling between local degrees of freedom in the simulation model are essential for accurate modeling of the structural ensemble. To address this challenge, we draw an analogy between electronic transitions and transitions between conformational basins, in the context of surface-hopping techniques. Instead of matching the PES due to different types of electronic configurations, we aim to reproduce features of distinct conformational basins of the underlying free-energy surface. Thus, we assign distinct force fields to conformations belonging to a given basin, and hop between conformationally-dependent surfaces. Rather than hop between surfaces in a stochastic manner, we ascribe a continuous-switching scheme. In contrast to previous studies employing discrete transitions between distinct force fields, the transitions between local conformational basins considered in this work occur on comparable timescales to the local dynamics, discouraging the use of the Monte Carlo approaches. Surface-hopping schemes for chemical reactions typically weight each surface according to solutions of the Schrödinger equation, effectively leading to a strong dependence on the relative energies. Because we aim at reproducing the free energy of each conformational basin, we require

* bereau@mpip-mainz.mpg.de

an integrated measure. As such we define the weights using a structural criterion: a metric depending collectively on the instantaneous values of the order parameters governing each interaction. Despite retaining the standard molecular-mechanics form of individual force fields, the conformationally-dependent surface hopping generates complex cross-correlations between local degrees of freedom, as we will demonstrate below.

Methodology. Instead of relying on a single force field, we model a molecular system by means of n force fields, each focusing on specific conformational basins (Fig. 1). The splitting of conformational space is provided by a density-based cluster analysis applied along the CG interaction terms of interest [26]. The reference trajectories are then split according to cluster identities, allowing us to build n force fields using standard structure-based CG procedures (force-matching in the present work).

The i -th cluster describes a subset of conformational space projected down onto two CG interaction terms denoted x and y (Fig. 1)—for instance a bond and bending angle, as in the hexane application below. We further define the cluster center, $\mu^{(i)} = (\mu_x^{(i)}, \mu_y^{(i)})$, corresponding to a local maximum of probability density across each variable. Similarly, we define the spatial extent of the cluster by means of its standard deviation, $\sigma^{(i)} = (\sigma_x^{(i)}, \sigma_y^{(i)})$. We apply a linear transformation on the clusters to enhance their isotropy: $\bar{\sigma}^{(i)} = (\bar{\sigma}_x^{(i)}, \bar{\sigma}_y^{(i)})$.

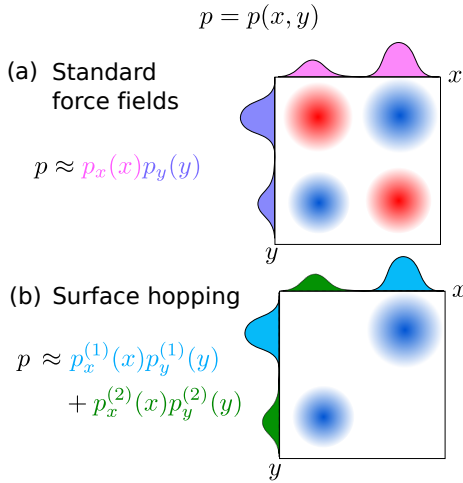


FIG. 1. Consider a 2D potential $U = U(x, y)$ leading to the distribution $p = p(x, y)$ populated by two peaks (in blue). (a) Standard force fields apply a global separation of variables on the potential $U(x, y) \approx U(x) + U(y)$ such that $p \approx p_x(x)p_y(y)$ leading to two spurious peaks (in red). (b) Surface hopping retains the separation of variables, but determines a local force field per conformational basin.

Force field i is characterized by its potential energy, $U_i(\mathbf{R})$, and corresponding force $\mathbf{f}_i(\mathbf{R}) = -\nabla U_i(\mathbf{R})$. Force field i is assigned a coefficient w_i that weights its instantaneous contribution, such that the net force on any par-

ticle is a weighted sum over all force fields

$$\mathbf{f}(\mathbf{R}) = \sum_{i=1}^n w_i \mathbf{f}_i(\mathbf{R}). \quad (1)$$

The weight w_i of force field i is determined by the Euclidean distance between the system's instantaneous configuration along the CG interaction variables (x, y) and the center of the i -th cluster $d_i^2 = (x - \mu_x^{(i)})^2 / \bar{\sigma}_x^{(i)} + (y - \mu_y^{(i)})^2 / \bar{\sigma}_y^{(i)}$, where the scaling by $\bar{\sigma}_{x,y}^{(i)}$ normalizes the contribution of each interaction. This distance is compared to the spatial extent of the cluster through the norm $|\bar{\sigma}^{(i)}|$. If the system is within the cluster's spatial extent its force field gets full weight, otherwise we suppress the weight exponentially

$$w_i = \begin{cases} 1, & d_i < |\bar{\sigma}^{(i)}| \\ \exp\left(-\frac{d_i - |\bar{\sigma}^{(i)}|}{\alpha}\right), & \text{otherwise.} \end{cases} \quad (2)$$

The scaling factor α smoothly dampens the contribution of force field i to avoid numerical instabilities upon integrating the equations of motion. A value of α that is small compared to the spatial extent of any cluster center avoids the blurring of the different PESs.

The mixing of several force fields, as described in Eqn. 1, can easily lead to unphysical behavior, even from a weak contribution of a surface containing large restoring forces. To avoid such a behavior, we restrict the mixing as much as possible. This is achieved by defining the first $n - 1$ surfaces that are localized to a cluster center, while the last force field n embodies the default option. This fallback surface is thus *not* associated to any cluster center, but instead parametrized from the rest of the trajectory that has not yet been considered. We compute the weights w_i (Eqn. 2) for the first $n - 1$ surfaces, keep only the one with the largest contribution $w_l = \max_{i < n} w_i$, and assign the rest of the weight to the fallback surface, $w_n = 1 - w_l$. As such, the surface mixing described in Eqn. 1 is always limited to the closest cluster center and the fallback force field. When the system is far from any cluster center, it relies solely on the fallback surface ($w_n = 1$). Our scheme directly hops between surfaces without rescaling velocities, and thereby violates total-energy conservation. In the canonical ensemble the thermostat is capable of absorbing a certain amount of energy violation [25], which we enhance by working at high friction.

While the algorithm described above yields surface hopping, it doesn't ensure the correct probabilities of sampling each surface. To this end, the ultra coarse-graining framework matches the transition rates through a self-consistent optimization [25]. Here we simply enforce the system to sample each surface i such that the time average $\langle w_i \rangle$, taken as a proxy of its canonical probability, matches the target probability p_i —available upon partitioning of the conformational space. The matching is enforced by locking the system that is currently vis-

iting surface i on that force field until $\langle w_i \rangle \approx p_i$. In practice, we let the system escape from surface i once $\langle w_i \rangle \geq 0.98 p_i$. While we only constrain a lower bound on sampling each surface, our experience so far indicates that it is sufficient to recover the correct probabilities.

All simulation details are described in the Supplemental Material (SM) [27]. An implementation of the surface-hopping scheme is available in ESPRESSO++ [28], as well as all simulation and analysis scripts [29].

Hexane. We first consider a single hexane molecule in vacuum coarse-grained to 3 beads—a challenging case despite its apparent simplicity. The CG potential employed bonded interactions between subsequent pairs of beads along the chain and an angle-bending interaction between the three beads. This CG model was first described in Rühle *et al.* [30]. The force-matching-based multiscale coarse-graining (MS-CG) method applied to the reference all-atom (AA) trajectory led to significant structural discrepancies, as seen in the 1-dimensional bending-angle distribution (Fig. 2b). MS-CG overpopulates small-angle states ($100^\circ < \theta < 120^\circ$), while underpopulating the high-angle states ($\theta > 150^\circ$). Rudzinski and Noid later demonstrated that these discrepancies arise due to bond-angle cross-correlations that cannot be reproduced with the molecular-mechanics interaction set [31]. They applied an iterative generalized Yvon-Born-Green (iter-gYBG) scheme to reproduce the independent bond and bending-angle reference AA distributions, albeit at the cost of accuracy in the cross-correlations. The discrepancies in the cross-correlations between bond and bending angle generated by these models is illustrated by the free-energy surfaces (FESs) in Fig. 3. The AA model displays a complex surface made of four major minima, located asymmetrically on the surface. The symmetry of the iter-gYBG model, on the other hand, clearly illustrates the additivity of the interactions in the Hamiltonian: all large-bond states are more populated than the small-bond states, irrespective of the angle.

A clustering of conformational space in two surfaces (i.e., 2S model) leads to: (2S-1) the highest angle state coupling to the large bond state (cluster center: $b = 0.26$ nm, $\theta = 170^\circ$) and the fallback surface (2S-2). Fig. 2a shows how a 3-state CG model discriminates between: (3S-1) the highest angle state—identical to 2S-1; (3S-2) two intermediate angles ($\theta \approx 125^\circ$, $\theta \approx 155^\circ$) with large bond; and the fallback surface (3S-3): an intermediate and a low angle state ($\theta \approx 155^\circ$, $\theta \approx 105^\circ$) around both small and large bond states.

Fig. 2b displays the bending-angle canonical distributions for the different CG models. We find that 2S and 3S systematically refine the agreement with the AA distribution as compared to MS-CG: they lower the artificially large populations of small-angle states and increase the artificially-low populations of high-angle states. The 3S model reproduces the AA angle distribution remarkably accurately, with only a slightly-low population around $\theta \approx 105^\circ$. In addition, the interaction potentials become

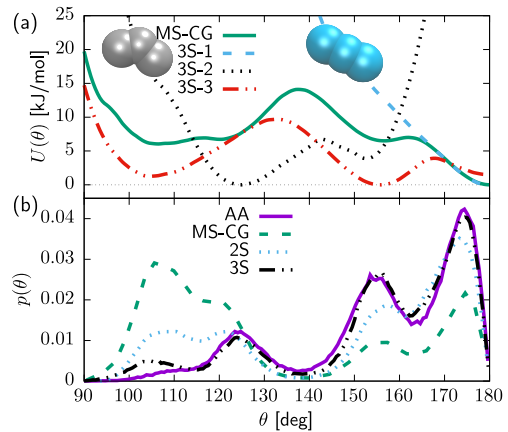


FIG. 2. Bending-angle properties of the CG hexane molecule. (a) Potential energy from force matching (MS-CG) and the three contributions of the 3-surface (3S) model. Cartoons display representative structures of the low-energy states for the relevant surface. (b) Probability distribution from the all-atom distribution projected onto CG variables (AA), force matching (MS-CG), and surface hopping with 2 (2S) and 3 (3S) force fields.

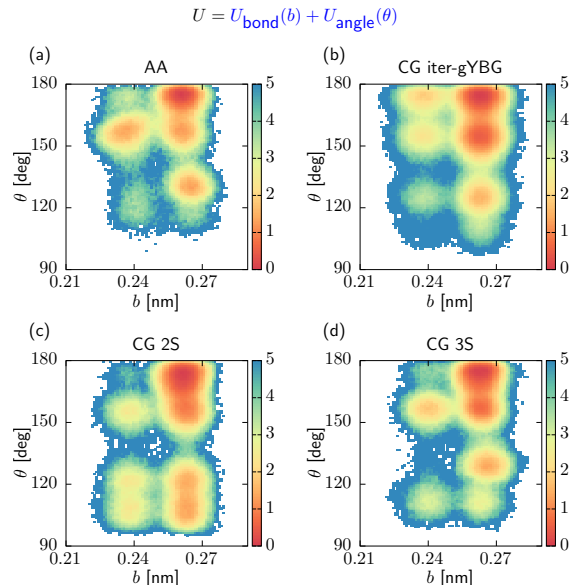


FIG. 3. Free-energy surfaces of the hexane molecule as a function of the bond, b , and bending angle, θ . (a) Reference surface; (b) CG iterative gYBG, (c) CG 2-state and (d) CG 3-state surfaces. Surface hopping couples bond with bending angle. Free energies expressed in $k_B T$.

more localized: while the MS-CG potential is extremely broad, the different 3S potentials are better confined.

The effect of the surface hopping technique is even more apparent in the FES. The 2S model demonstrates significant improvement relative to the standard molecular-mechanics force field by more accurately rep-

representing the heterogeneous populations of high-angle states. The 3S model further corrects the populations, especially for the low-angle states.

A Markov state model analysis [32, 33] of both the AA and different CG models yielded a lag time too close to the longest timescales to make use of the results, indicating that the dynamics are governed by diffusive behavior and lack timescale separation between the conformational basins.

Tetraalanine: As a second system, we consider Ala₄, a tetraalanine peptide made of 52 atoms solvated in water, coarse-grained to only four beads [34]. Each bead was placed at the position of the alpha carbon on the peptide backbone. The CG force field employed bonded interactions between subsequent pairs of sites along the peptide chain, two angle-bending interactions, θ , a dihedral interaction, ψ , and an additional effective bond between the terminal beads of the chain, R_{1-4} .

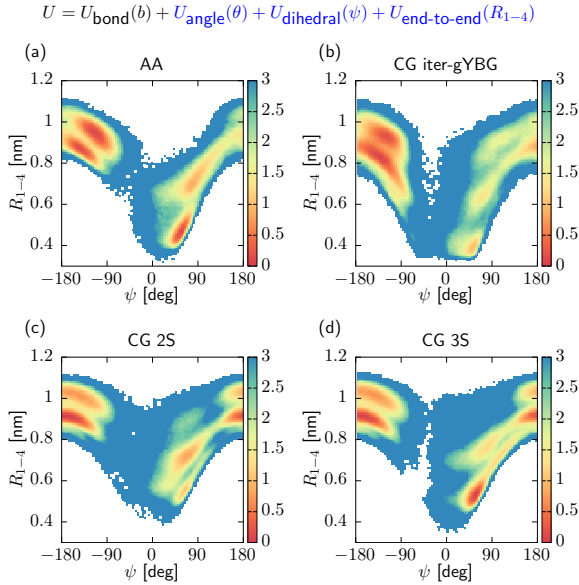


FIG. 4. Free-energy surfaces of Ala₄ as a function of the dihedral, ψ , and end-to-end distance, R_{1-4} . (a) Reference surface; (b) CG iterative gYBG, (c) CG 2-state and (d) CG 3-state surfaces. Surface hopping couples the bending angle, dihedral, and the effective R_{1-4} interaction. Free energies expressed in $k_B T$.

Both MS-CG and iter-gYBG models displayed two notable discrepancies on the FES (Fig. 4 and SM): a spurious region of intermediates ($\psi \approx 90^\circ$, $R_{1-4} \approx 0.9$ nm) and the extended state stabilized at too large dihedrals ($\psi \approx -90^\circ$, $R_{1-4} \approx 0.6$ nm). Surface-hopping models that couple θ , ψ , and R_{1-4} using 2 and 3 surfaces suppress both regions. Further, a 4S model (SM) shows structural accuracy on par with 3S. The results highlight the capability of the surface-hopping scheme to introduce cross-correlations beyond the additivity assumption of the Hamiltonian. This improvement is due not only to the introduction of cross-correlations between in-

teractions, but also to the simplification of the target surface when determining each force field. In particular, we have found that as the number of surfaces increases, the distributions within each basin become increasingly unimodal, resulting in very simple interaction potentials and systematically improving the accuracy of the model.

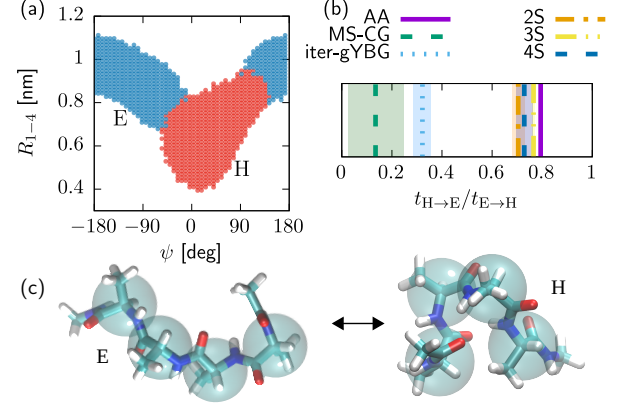


FIG. 5. (a) Basin decomposition between helical (H) and extended (E) states. (b) Ratio of mean-first-passage times between the helical and extended states, $t_{H \rightarrow E}/t_{E \rightarrow H}$. (c) Cartoon representations of the extended and helical states.

Beyond structural properties, the dynamics also show significant improvements. We monitor the transition kinetics between the helical (H) and extended (E) metastable basins (Fig. 5a and c), identified from a Markov state model analysis of the reference AA simulation [34, 35]. We focus on *ratios* of mean-first-passage times to factor out any homogeneous speedup factor due to coarse-graining. Compared with the MS-CG and iter-gYBG models, the ratios of mean-first-passage times converge more consistently over a wider range of characteristic timescales, indicating better-defined kinetic boundaries between conformational basins. The surface hopping schemes also yield significantly better agreement with the AA result (Fig. 5b). We observe a systematic improvement for the different surface-hopping models, where both 3S and 4S lie almost within the error bars of the reference AA observable. The results indicate that not only are the free-energy barriers well reproduced, the diffusive behavior in the different basins is consistently sped up.

Achieving consistent long-time dynamics of a tetraalanine peptide solvated in water using only four beads is remarkable, given the tendency of CG models to display severe kinetic discrepancies [2]. In previous studies, kinetically-consistent CG models have only been systematically achieved using a Mori-Zwanzig formalism, where a generalized Langevin equation introduces a computationally-expensive memory kernel to account for the degrees of freedom coarse-grained away [36]. Here, our results demonstrate that a simple model solely parametrized against structural properties can quantita-

tively reproduce the long time-scale dynamics. Indeed, the model’s accurate description of the free-energy barriers enforces the barrier-crossing dynamics, akin to Marcus theory for electron-transfer reactions [37]. On the other hand, local diffusion within a conformational basin remain inconsistent because of reduced molecular friction [35]. Our findings generalize beyond coarse-graining: surface-hopping models offer a systematic method to achieve accurate barrier-crossing dynamics, but the quality of the local diffusion is inherently limited by the physics of the model. Empirical valence bond models showed a strong dependence of the quality of the individual surfaces on excess proton dynamics [38]. Systems

whose kinetics are dominated by activated processes can thus be accurately characterized with remarkably simple force fields, unlike in the diffusive regime.

ACKNOWLEDGMENTS

We thank Denis Andrienko, Burkhard Dünweg, Kurt Kremer, and Clemens Rauer for insightful discussions. This work was supported in part by the TRR 146 Collaborative Research Center of the Deutsche Forschungsgemeinschaft (DFG), the Emmy Noether program to TB and a postdoctoral fellowship from the Alexander von Humboldt foundation to JFR.

-
- [1] T. Murtola, A. Bunker, I. Vattulainen, M. Deserno, and M. Karttunen, *Physical Chemistry Chemical Physics* **11**, 1869 (2009).
 - [2] C. Peter and K. Kremer, *Soft Matter* **5**, 4357 (2009).
 - [3] C. Peter and K. Kremer, *Faraday discussions* **144**, 9 (2010).
 - [4] S. C. Kamerlin, S. Vicatos, A. Dryga, and A. Warshel, *Annual review of physical chemistry* **62**, 41 (2011).
 - [5] S. O. Nielsen, C. F. Lopez, G. Srinivas, and M. L. Klein, *Journal of Physics: Condensed Matter* **16**, R481 (2004).
 - [6] G. A. Voth, *Coarse-graining of condensed phase and biomolecular systems* (CRC press, 2008).
 - [7] E. Brini, E. A. Algaer, P. Ganguly, C. Li, F. Rodríguez-Ropero, and N. F. van der Vegt, *Soft Matter* **9**, 2108 (2013).
 - [8] W. Noid, *The Journal of chemical physics* **139**, 09B201.1 (2013).
 - [9] W. Noid, J.-W. Chu, G. S. Ayton, V. Krishna, S. Izvekov, G. A. Voth, A. Das, and H. C. Andersen, *The Journal of chemical physics* **128**, 244114 (2008).
 - [10] J. F. Rudzinski and W. Noid, *The Journal of chemical physics* **135**, 214101 (2011).
 - [11] W. Tschöp, K. Kremer, J. Batoulis, T. Bürger, and O. Hahn, *Acta Polymerica* **49**, 61 (1998).
 - [12] W. Noid, P. Liu, Y. Wang, J.-W. Chu, G. S. Ayton, S. Izvekov, H. C. Andersen, and G. A. Voth, *The Journal of chemical physics* **128**, 244115 (2008).
 - [13] M. S. Shell, *The Journal of chemical physics* **129**, 144108 (2008).
 - [14] V. Molinero and E. B. Moore, *The Journal of Physical Chemistry B* **113**, 4008 (2008).
 - [15] T. Sanyal and M. S. Shell, *The Journal of Physical Chemistry B* **122**, 5678 (2018).
 - [16] S. T. John and G. Csányi, *The Journal of Physical Chemistry B* **121**, 10934 (2017).
 - [17] A. Warshel and R. M. Weiss, *Journal of the American Chemical Society* **102**, 6218 (1980).
 - [18] U. W. Schmitt and G. A. Voth, *The Journal of Physical Chemistry B* **102**, 5547 (1998).
 - [19] J. C. Tully, *The Journal of Chemical Physics* **93**, 1061 (1990).
 - [20] T. Murtola, M. Karttunen, and I. Vattulainen, *J. Chem. Phys.* **131**, 55101 (2009).
 - [21] V. C. Chappa, D. C. Morse, A. Zippelius, and M. Müller, *Physical Review Letters* **109**, 1 (2012).
 - [22] M. Knott and R. B. Best, *The Journal of chemical physics* **140**, 05B603.1 (2014).
 - [23] I. Pagonabarraga and D. Frenkel, *The Journal of Chemical Physics* **115**, 5015 (2001).
 - [24] J. F. Dama, A. V. Sinitskiy, M. McCullagh, J. Weare, B. Roux, A. R. Dinner, and G. A. Voth, *Journal of chemical theory and computation* **9**, 2466 (2013).
 - [25] A. Davtyan, J. F. Dama, A. V. Sinitskiy, and G. A. Voth, *Journal of chemical theory and computation* **10**, 5265 (2014).
 - [26] F. Sittel and G. Stock, *Journal of chemical theory and computation* **12**, 2426 (2016).
 - [27] See Supplemental Material [URL] for simulation details; generation of the CG potentials; free-energy surfaces; and Markov state model analysis, which includes Refs. [39–51].
 - [28] J. D. Halverson, T. Brandes, O. Lenz, A. Arnold, S. Bevc, V. Starchenko, K. Kremer, T. Stuehn, and D. Reith, *Computer Physics Communications* **184**, 1129 (2013).
 - [29] https://gitlab.mpcdf.mpg.de/trisb/cg_surf_hop, accessed August 1, 2018.
 - [30] V. Rühle, C. Junghans, A. Lukyanov, K. Kremer, and D. Andrienko, *Journal of Chemical Theory and Computation* **5**, 3211 (2009).
 - [31] J. F. Rudzinski and W. G. Noid, *Journal of Physical Chemistry B* **118**, 8295 (2014).
 - [32] F. Noé, *J. Comp. Phys.* **28**, 244103 (2008).
 - [33] G. R. Bowman, V. S. Pande, and F. Noé, *An Introduction to Markov State Models and Their Application to Long Timescale Molecular Simulation* (Springer Science and Business Media, Dordrecht, Netherlands, 2014).
 - [34] J. F. Rudzinski and W. G. Noid, *Journal of Chemical Theory and Computation* **11**, 1278 (2015).
 - [35] J. F. Rudzinski, K. Kremer, and T. Bereau, *The Journal of Chemical Physics* **144**, 051102 (2016).
 - [36] C. Hijón, P. Español, E. Vanden-Eijnden, and R. Delgado-Buscalioni, *Faraday discussions* **144**, 301 (2010).
 - [37] R. A. Marcus, *The Journal of Chemical Physics* **24**, 966 (1956).
 - [38] Y. Wu, H. Chen, F. Wang, F. Paesani, and G. A. Voth, *The Journal of Physical Chemistry B* **112**, 467 (2008).

- [39] A. Jain and G. Stock, [Journal of Chemical Theory and Computation](#) **8**, 3810 (2012).
- [40] W. L. Jorgensen, D. S. Maxwell, and J. Tirado-Rives, [J. Chem. Phys.](#) **118**, 11225 (1996).
- [41] H. Berendsen, J. Grigera, and T. Straatsma, [J. Phys. Chem.](#) **91**, 6269 (1987).
- [42] B. Hess, C. Kutzner, D. van der Spoel, and E. Lindahl, [J. Chem. Phys.](#) **127**, 122301 (2007).
- [43] S. Izvekov and G. A. Voth, [Journal of Physical Chemistry B](#) **109**, 2469 (2005).
- [44] S. Izvekov and G. A. Voth, [Journal of Chemical Physics](#) **123**, 134105 (2005).
- [45] W. G. Noid, J.-W. Chu, G. S. Ayton, and G. A. Voth, [Journal of Physical Chemistry B](#) **111**, 4116 (2007).
- [46] W. G. Noid, J.-W. Chu, G. S. Ayton, V. Krishna, S. Izvekov, G. A. Voth, A. Das, and H. C. Andersen, [Journal of Chemical Physics](#) **128**, 244114 (2008).
- [47] J. W. Mullinax and W. G. Noid, [Physical Review Letters](#) **103**, 198104 (2009).
- [48] J. W. Mullinax and W. G. Noid, [Journal of Physical Chemistry C](#) **114**, 5661 (2010).
- [49] C. R. Ellis, J. F. Rudzinski, and W. G. Noid, [Macromolecular Theory and Solutions](#) **20**, 478 (2011).
- [50] J.-H. Prinz, H. Wu, M. Sarich, B. Keller, M. Senne, M. Held, J. D. Chodera, C. Schütte, and F. Noé, [J. Comp. Phys.](#) **134**, 174105 (2011).
- [51] W. Humphrey, A. Dalke, and K. Schulten, [Journal of molecular graphics](#) **14**, 33 (1996).